mTORC1 mediated translational elongation limits intestinal tumour initiation and growth

William J. Faller[1], Thomas J. Jackson[2*], John RP Knight[2*], Rachel A. Ridgway[1], Thomas Jamieson[1], Saadia A. Karim[1], Carolyn Jones[2], Sorina Radulescu[1], David J. Huels[1], Kevin B. Myant[1], Kate M. Dudek[2], Helen A. Casey[1], Mario Pende[3], Alexey G. Ryazanov[4], Nahum Sonenberg[5], Oded Meyuhas[6], Michael N. Hall[7], Martin Bushell[2], Anne E. Willis[2], Owen J. Sansom[1].

Abstract

Inactivation of APC is a strongly predisposing event in the development of colorectal cancer[1,2], prompting us to search for vulnerabilities specific to cells that have lost APC function. Signalling through the mTOR pathway is known to be required for epithelial cell proliferation and tumour growth[3-5] and the current paradigm suggests that a critical function of mTOR activity is to upregulate translational initiation through phosphorylation of 4EBP1[6,7]. This model predicts that the mTOR inhibitor rapamycin, which does not efficiently inhibit 4EBP1[8], would be ineffective in limiting cancer progression in APC deficient lesions. Here we show that mTORC1 activity is absolutely required for the proliferation of APC deficient (but not wild type) enterocytes, revealing an unexpected opportunity for therapeutic intervention. Although APC deficient cells show the expected increases in protein synthesis, our studies reveals that it is translation elongation, and not initiation, which is the rate-limiting component. Mechanistically, mTORC1 mediated inhibition of eEF2 kinase is required for the proliferation of APC deficient cells. Importantly, treatment of established APC deficient adenomas with rapamycin (which can target eEF2 through the mTORC1 – S6K – eEF2K axis) causes tumour cells to undergo growth arrest and differentiation. Taken

together our data suggest that inhibition of translation elongation using existing, clinically approved drugs such as the Rapalogs, would provide clear therapeutic benefit for patients at high-risk of developing colorectal cancer.

Main Text

The ability of the intestinal epithelium to regenerate following challenge has been well described[9-11]. We have shown that this is a Wnt-driven process that mimics the proliferation observed following *Apc* deletion[11,12] and is a valuable model of the early stages of intestinal cancer. However, the underlying mechanisms controlling these processes are largely unknown. The serine/threonine kinase mTOR, particularly the mTOR Complex 1 (mTORC1), is a known mediator of cell growth and proliferation[13]. Previous studies have suggested that mTORC1 may be important in both the intestinal stem-cell niche and for intestinal tumourigenesis[4,5,14]. We therefore queried the role of mTORC1 in intestinal proliferation following Wnt activation. Following *Apc* deletion there was an increase in the phosphorylation status of mTORC1 effectors rpS6 and 4EBP1 that was dependent on MYC expression. Increased phosphorylation of these proteins was also seen during crypt regeneration (Fig. 1a,b,c, Extended Data Fig. 1a). Importantly, the mTOR inhibitor rapamycin blocked intestinal regeneration, demonstrating that mTOR signalling is required for this process (Fig. 1d,e). Given that rapamycin did not affect apoptosis nor proliferation in the normal intestine (Extended Data Fig. 1b,c), these data suggest that there may be a potential therapeutic window, between normal intestinal enterocytes and those with a high level of Wnt activity. Therefore Raptor (an essential component of mTORC1) was deleted in the intestinal epithelium (Extended Data Fig. 1d). Surprisingly, normal gut homeostasis was unaffected by Raptor loss 4 days post-Cre induction, when using an epithelium-specific Cre-Recombinase (*VillinCRE*^{ER} *Rptor*$^{fl/fl}$) (Extended Data Fig. 1e,f). Furthermore, 400 days after induction, no phosphorylation of rpS6 or 4EBP1 was observed, showing that Raptor deletion was sustained (Extended Data Fig. 2a). Raptor loss caused no change in either levels of mitosis or apoptosis (Extended Data Fig. 2b,c) but proved to be essential for the proliferative phenotype observed during regeneration or following *Apc* deletion (Fig. 1a,b,d,e,f). Nuclear

localisation of β-catenin and high levels of MYC could be demonstrated by IHC, showing that Wnt-activation is still present (Extended Data Fig. 3a,b).

Given that rapamycin treatment and Raptor deletion had similar effects, we examined whether rapamycin treatment was sufficient to modify intestinal tumourigenesis, either prophylactically, or chemotherapeutically. First we assessed whether rapamycin could suppress a model of intestinal tumourigenesis, in which *Apc* deletion is targeted to LGR5-positive stem cells using the *LGR5CRE*^{ER} (*LGR5CRE*^{ER} *Apc*$^{fl/fl}$). Mice were treated starting 10 days post-Cre induction, and in contrast to controls, remained tumour free for the duration of the experiment (Fig. 2a,b). Next we treated mice (*Apc*$^{Min/+}$ or *LGR5CRE*^{ER} *Apc*$^{fl/fl}$) with established adenomas. Remarkably, the mice lost their clinical symptoms of disease and survived significantly longer than controls (Fig. 2c,d; Extended Data Fig. 4a). We next analysed the tumours from these mice over a time-course post-rapamycin treatment. Treatment caused a loss of proliferation specifically within the tumours by 72-hours, and an increase in the number of Lysozyme-positive paneth cells (Fig. 2e; Extended Data Fig. 4b,c). By 30 days, most tumours had shrunk considerably to small non-proliferative lesions that no longer contained paneth cells (Fig. 2f; Extended Data Fig. 4d). Within the normal intestine there are two main cell populations that show high levels of Wnt-signalling; the label-retaining/progenitor population and the paneth cell population[15]. Our data suggest that treatment of mice with rapamycin causes the differentiation of the tumour's Wnt-high progenitor cells into the other Wnt-high fate in the intestine; namely non-proliferative paneth-like cells. The cell-cycle arrest in these cells was examined by staining for p21, p16, p53. No increase in these markers was observed, suggesting a classical cell cycle arrest pathway had not been engaged (Extended Data Fig. 5a). We reasoned that if mice were removed from rapamycin the tumours would regain proliferative capacity. Indeed, when rapamycin

treatment was halted, signs of intestinal neoplasia were observed approximately 40–60 days later (Extended Data Fig. 4a). This suggested that intestinal adenoma stem cells were still present. Tumours from *LGR5-GFP-CRE*^{ER} mice were stained to detect *LGR5-GFP* positivity. We found that following rapamycin treatment, numerous LGR5-positive cells were still present, indicating that, while rapamycin treatment causes a regression of the lesions, the tumour initiating cells remain (Extended Data Fig. 5b).

We examined the mechanism of mTORC1 requirement following *Apc* loss. mTORC1 is known to regulate protein synthesis on multiple levels and most research has focused on two downstream effectors: 4EBP1 and S6K. A number of studies have suggested that translation initiation, via the 4EBP1 – eIF4E axis, is the critical effector of mTOR in cancer[6,16]. However, it has been shown that rapamycin preferentially inhibits the phosphorylation of S6K over 4EBP1[8], suggesting that 4EBP1-mediated inhibition of translation initiation may not be limiting in the context of *Apc* loss. To assess the changes in translational control in response to mTORC1 inhibition, we measured the polysomal distribution in WT, *Apc*-deficient and *Apc/*Raptor-deficient intestinal epithelial cells 4-days post gene deletion. *Apc* deletion resulted in a decrease in the number of polysomes, whereas *Apc/*Raptor co-deletion reversed this effect (Fig. 3a). The decrease in the number of polysomes following *Apc* deletion could suggest either reduced translation initiation (and consequently a lower overall level of translation) and/or a faster rate of translational elongation. Global translation rates were measured using an *in vitro* intestinal crypt 3d-culture model[17]. The *Apc*-deficient cells were shown to have increased ^{35}S-labelled methionine/cysteine incorporation compared to WT, showing higher overall levels of protein synthesis (Fig. 3b). Unfortunately, Raptor deletion prevented the growth of crypts *in vitro* so this could not be assayed (Extended Data Fig. 6).

To measure the rate of translational elongation, an *in vitro* harringtonine run-off assay was performed[18], as described in Supplementary Materials and Methods. There was a >2.5-fold increase in ribosome run-off in crypts with *Apc* deletion compared to wild-type (Fig. 3c; Extended Data Fig. 7). This suggests that following Wnt activation, elongation, rather than initiation, is rate limiting for protein synthesis and mTORC1 must be activated to overcome this.

Cycloheximide (an inhibitor of elongation[19]) reduced proliferation associated with *Apc* deletion, to a similar level to rapamycin (Extended Data Fig. 8). While cycloheximide is acknowledged to inhibit elongation[19], it must be emphasised that 72hr treatment could result in broad alterations in protein synthesis. However, the $Apc^{fl/fl}$-specific loss of proliferation observed here provides "proof of principle" to demonstrate that modulation of protein synthesis may be useful as a chemotherapeutic strategy.

As most previous work has suggested translation initiation downstream of 4EBP1 is limiting to cancer[20], it was important to probe known effectors of mTORC1 in this system. Given the alteration of elongation rates, the elongation factor 2 kinase (eEF2K), a known target of S6K[21,22] was of particular interest. eEF2K is a negative regulator of the elongation factor 2 (eEF2), giving mTORC1 the ability to promote translational elongation via S6K[23]. Using multiple mouse knockout and knock-in alleles, we further dissected the downstream effectors of mTORC1 in intestinal regeneration. *S6k1/2* knockout decreased intestinal regeneration, whilst knockout of *Eif4ebp1/2* had no effect. As the 4EBP proteins are negative regulators of eIF4E, an increase (rather than decrease) in regeneration may have been predicted, but this was not found. Moreover these intestines were still sensitive to rapamycin, demonstrating that

rapamycin was acting via the mTORC1-S6K branch rather than 4EBP1-eIF4E (Extended Data Fig. 9). We then used an *Eef2k*-null mouse and showed that following irradiation and treatment with rapamycin, these mice were now resistant to mTORC1 inhibition, confirming the importance of translational elongation (Fig. 4a). To ensure that S6K was not also acting through its more established effector, rpS6, we used an *rpS6* phospho-mutant that cannot be phosphorylated by S6K. This was unable to phenocopy Raptor deletion (Fig. 4a), showing that Wnt-driven regeneration requires increased translational elongation, mediated through mTORC1.

To prove that inhibition of eEF2K by S6K is required to allow increased eEF2 activity following *Apc* loss, we intercrossed *VillinCRE*^{ER} *Apc*$^{fl/fl}$ to *Eef2k*$^{-/-}$ mice and treated these with rapamycin. In contrast to *VillinCRE*^{ER} *Apc*$^{fl/fl}$ mice, these intestines were now resistant to growth inhibitory effects of rapamycin (Fig. 4b,c). Tellingly, these mice no longer show an increase in the inhibitory phosphorylation of eEF2 following rapamycin treatment (Extended Data Fig. 10).

To assess whether the increased elongation following *Apc* deletion had differential affects on cell cycle regulating proteins, RNA and protein levels of several key cell cycle regulators were tested (Fig. 4d,e). This analysis revealed that whilst there were increased RNA and protein levels of Cyclin D1, D2, CDK4 and CDK6, Cyclin D3 had increased protein levels in the absence of increased mRNA levels. Cyclin D3 protein levels were sensitive to rapamycin exposure, and this sensitivity depends on eEF2K (Extended Data Fig. 11). Additionally, ribosomes were shown to elongate approximately 4-times faster on Cyclin D3 messages in *Apc*-deficient cells than WT cells. No differences were detected in other messages tested (Extended Data Fig. 12). Taken together, these data suggest that Cyclin D3 is translationally

regulated at the level of elongation, consistent with previous reports[24,25]. The contribution of Cyclin D3 to the proliferative phenotype remains to be elucidated.

In summary, we report that mTORC1 is an essential downstream effector of Wnt-signalling in the intestine. We show that intestinal proliferation associated with Wnt-signalling requires the mTORC1 – S6K – eEF2K – eEF2 axis, and that the resulting increase in the rate of elongation of specific polypeptides overcomes a limiting translational step. Our work highlights key functional roles for eEF2K and translational elongation in the control of the initiation of cancer and adenomatous proliferation. The importance of elongation in this context has been suggested in a small number of publications, but this study provides definitive *in vivo* evidence[26-28]. Finally, we have also shown that targeting mTOR and translational control may be a viable strategy for chemoprevention of CRC in high risk patients, and treatment of early stage disease. Indeed, recent studies have suggested that the chemopreventative agents aspirin and mesalazine also target mTOR[29,30].

1 Kinzler, K. W. & Vogelstein, B. Lessons from hereditary colorectal cancer. Cell 87, 159-170 (1996).

2 Korinek, V. et al. Constitutive transcriptional activation by a beta-catenin-Tcf complex in APC-/- colon carcinoma. Science 275, 1784-1787 (1997).

3 Ashton, G. H. et al. Focal adhesion kinase is required for intestinal regeneration and tumorigenesis downstream of Wnt/c-Myc signaling. Developmental cell 19, 259-269, doi:10.1016/j.devcel.2010.07.015 (2010).

4 Fujishita, T., Aoki, K., Lane, H. A., Aoki, M. & Taketo, M. M. Inhibition of the mTORC1 pathway suppresses intestinal polyp formation and reduces mortality in ApcDelta716 mice. Proceedings of the National Academy of Sciences of the United States of America 105, 13544-13549, doi:10.1073/pnas.0800041105 (2008).

5 Gulhati, P. et al. Targeted inhibition of mammalian target of rapamycin signaling inhibits tumorigenesis of colorectal cancer. Clin Cancer Res 15, 7207-7216, doi:10.1158/1078-0432.CCR-09-1249 (2009).

6 Pourdehnad, M. et al. Myc and mTOR converge on a common node in protein synthesis control that confers synthetic lethality in Myc-driven cancers.

Proceedings of the National Academy of Sciences of the United States of America 110, 11988-11993, doi:10.1073/pnas.1310230110 (2013).

7 Martineau, Y. et al. Pancreatic tumours escape from translational control through 4E-BP1 loss. Oncogene, doi:10.1038/onc.2013.100 (2013).

8 Jiang, Y. P., Ballou, L. M. & Lin, R. Z. Rapamycin-insensitive regulation of 4e-BP1 in regenerating rat liver. J Biol Chem 276, 10943-10951, doi:10.1074/jbc.M007758200 (2001).

9 Bach, S. P., Renehan, A. G. & Potten, C. S. Stem cells: the intestinal stem cell as a paradigm. Carcinogenesis 21, 469-476 (2000).

10 Bernal, N. P. et al. Evidence for active Wnt signaling during postresection intestinal adaptation. Journal of pediatric surgery 40, 1025-1029; discussion 1029, doi:10.1016/j.jpedsurg.2005.03.021 (2005).

11 Ireland, H. et al. Inducible Cre-mediated control of gene expression in the murine gastrointestinal tract: effect of loss of beta-catenin. Gastroenterology 126, 1236-1246 (2004).

12 Muncan, V. et al. Rapid loss of intestinal crypts upon conditional deletion of the Wnt/Tcf-4 target gene c-Myc. Molecular and cellular biology 26, 8418-8426, doi:10.1128/MCB.00821-06 (2006).

13 Zoncu, R., Efeyan, A. & Sabatini, D. M. mTOR: from growth signal integration to cancer, diabetes and ageing. Nat Rev Mol Cell Biol 12, 21-35, doi:10.1038/nrm3025 (2011).

14 Yilmaz, O. H. et al. mTORC1 in the Paneth cell niche couples intestinal stem-cell function to calorie intake. Nature 486, 490-495, doi:10.1038/nature11163 (2012).

15 Farin, H. F., Van Es, J. H. & Clevers, H. Redundant sources of Wnt regulate intestinal stem cells and promote formation of Paneth cells. Gastroenterology 143, 1518-1529 e1517, doi:10.1053/j.gastro.2012.08.031 (2012).

16 She, Q. B. et al. 4E-BP1 is a key effector of the oncogenic activation of the AKT and ERK signaling pathways that integrates their function in tumors. Cancer Cell 18, 39-51, doi:10.1016/j.ccr.2010.05.023 (2010).

17 Sato, T. et al. Single Lgr5 stem cells build crypt-villus structures in vitro without a mesenchymal niche. Nature 459, 262-265, doi:10.1038/nature07935 (2009).

18 Fresno, M., Jimenez, A. & Vazquez, D. Inhibition of translation in eukaryotic systems by harringtonine. European journal of biochemistry / FEBS 72, 323-330 (1977).

19 Schneider-Poetsch, T. et al. Inhibition of eukaryotic translation elongation by cycloheximide and lactimidomycin. Nat Chem Biol 6, 209-217, doi:10.1038/nchembio.304 (2010).

20 ***Hsieh, A. C. et al. The translational landscape of mTOR signalling steers cancer initiation and metastasis. Nature 485, 55-61, doi:10.1038/nature10912 (2012).***

21 ***Richter, J. D. & Sonenberg, N. Regulation of cap-dependent translation by eIF4E inhibitory proteins. Nature 433, 477-480, doi:10.1038/nature03205 (2005).***

22 ***Browne, G. J. & Proud, C. G. A novel mTOR-regulated phosphorylation site in elongation factor 2 kinase modulates the activity of the kinase and its binding to calmodulin. Molecular and cellular biology 24, 2986-2997 (2004).***

23 ***Ryazanov, A. G., Shestakova, E. A. & Natapov, P. G. Phosphorylation of elongation factor 2 by EF-2 kinase affects rate of translation. Nature 334, 170-173, doi:10.1038/334170a0 (1988).***

24 ***Gorshtein, A. et al. Mammalian target of rapamycin inhibitors rapamycin and RAD001 (everolimus) induce anti-proliferative effects in GH-secreting pituitary tumor cells in vitro. Endocr Relat Cancer 16, 1017-1027, doi:10.1677/ERC-08-0269 (2009).***

25 ***Gutzkow, K. B. et al. Cyclic AMP inhibits translation of cyclin D3 in T lymphocytes at the level of elongation by inducing eEF2-phosphorylation. Cell Signal 15, 871-881 (2003).***

26 ***Firczuk, H. et al. An in vivo control map for the eukaryotic mRNA translation machinery. Mol Syst Biol 9, 635, doi:10.1038/msb.2012.73 (2013).***

27 ***Hussey, G. S. et al. Identification of an mRNP complex regulating tumorigenesis at the translational elongation step. Mol Cell 41, 419-431, doi:10.1016/j.molcel.2011.02.003 (2011).***

28 ***Nakamura, J. et al. Overexpression of eukaryotic elongation factor eEF2 in gastrointestinal cancers and its involvement in G2/M progression in the cell cycle. Int J Oncol 34, 1181-1189 (2009).***

29 ***Din, F. V. et al. Aspirin inhibits mTOR signaling, activates AMP-activated protein kinase, and induces autophagy in colorectal cancer cells. Gastroenterology 142, 1504-1515 e1503, doi:10.1053/j.gastro.2012.02.050 (2012).***

30 ***Baan, B. et al. 5-Aminosalicylic acid inhibits cell cycle progression in a phospholipase D dependent manner in colorectal cancer. Gut 61, 1708-1715, doi:10.1136/gutjnl-2011-301626 (2012).***

Extended Data is linked to the online version of the paper at **www.nature.com/nature**.

Acknowledgements

WJF is funded by AICR. OJS is funded by CRUK, ERC Investigator Grant (COLONCAN) and the European Union Seventh Framework Programme FP7/2007-2013 under grant

agreement number 278568. MB is an MRC Senior Fellow. Authors acknowledge Patrizia Cammareri and Claudio Murgia for proof reading of the manuscript.

Author contributions

OJS, AEW and WJF designed the project. WJF, RR, TJ and SR performed breeding and phenotypic analysis of mice; WJF, TJJ and JRPK performed translational analysis; MNH, AGR, NS, OM, DJH, KBM, SAK, KMD, CJ, HAC and MP provided advice and material; WJF, OJS, AEW and MB wrote and edited the manuscript.

Competing financial interests

The Authors declare no competing financial interests.

Figure 1: mTORC1 is essential for Wnt-driven proliferation in a MYC-dependent manner

a+b) Representative IHC of phospho-rpS6 and phospho-4EBP1 showing increased staining 96hrs following *Apc* deletion. Raptor deletion caused a loss of positivity in both, whereas 10mg/kg rapamycin treatment (beginning at 24hrs) specifically disrupts rpS6 phosphorylation; **c)** Representative IHC of phospho-rpS6 96hrs after Cre induction showing that Wnt-driven rpS6 phosphorylation is MYC dependent; **d)** Animals were exposed to 14Gy γ-irradiation and intestinal regeneration was measured 72hrs later, by counting the number of viable crypts and multiplying that by the average size of the regenerating crypts. Boxplot shows that 10mg/kg rapamycin treatment and Raptor deletion significantly decrease intestinal regeneration. Whiskers are max and min, black line is median (n=5 biological replicates per group; **p-value<0.02, Mann-Whitney U test); **e)** Representative H+E staining of regenerating intestines 72hrs after exposure to 14Gy γ-irradiation. Arrowheads indicate regenerating crypts; **f)** Representative H+E staining 96hrs after *Apc* loss, showing that 10mg/kg rapamycin treatment or Raptor deletion prevent Wnt-driven proliferation. Treatment

began 24hrs after *Apc* deletion. Red bar is graphical representation of crypt size. Scale bar = 100μm.

Figure 2: Apc-driven tumourigenesis requires mTORC1 activation

a+b) Graphical representation of prophylactic rapamycin treatment strategy and Kaplan-Meyer survival curve showing that prophylactic rapamycin treatment prevents tumourigenesis. 10mg/kg rapamycin treatment began at Day 10 post-*Apc* deletion, and lasted 30 days, after which mice were sampled. Area highlighted by red indicates duration of rapamycin treatment ($n \geq 7$; ***p-value$\leq$0.001, Log Rank test); **c+d)** Graphical representation of chemotherapeutic rapamycin treatment strategy and Kaplan-Meyer survival curve showing that rapamycin treatment can regress established intestinal tumours. 10mg/kg rapamycin treatment started when mice showed signs of intestinal disease, and lasted 30 days, after which mice were sampled. Graph represents survival while on rapamycin treatment ($n \geq 5$; ***p-value$\leq$0.001, Log Rank test); **e)** Representative IHC of phospho-rpS6, BrdU and Lysozyme, showing that 72hrs of 10mg/kg rapamycin treatment causes a loss in rpS6 phosphorylation and BrdU positivity, and an increase in lysozyme staining in intestinal tumours; **f)** Representative H+E and IHC for BrdU showing that small, non-proliferative lesions remain after 30 days of 10mg/kg rapamycin treatment. Scale bar = 100μm

Figure 3: mTORC1 drives increased translational elongation

a) Representative polysome profiles of intestinal epithelial cells showing altered RNA distribution 96hrs after *Apc* deletion. Bar graph represents the ratio of sub-polysomes compared to polysomes (S:P). Data are average ± s.e.m. ($n \geq 3$ per group; *p-value$\leq$0.05, Mann-Whitney U test); **b)** Intestinal crypt culture was pulsed for 30 min with ^{35}S-labelled methionine/cysteine. Incorporation of ^{35}S into protein was quantified by scintillation counting

and normalized to total protein. *Apc* deletion increases ^{35}S incorporation. Data are average ± s.e.m. (n=3 biological replicates per group; *p-value≤0.05, Mann-Whitney U test); **c)** The ribosome run-off rate was measured by addition of the initiation inhibitor harringtonine to *ex vivo* crypts from wild-type and *Apc* deleted mice. Harringtonine was added for 0 or 180 seconds and the increase in sub-polysomes (S) relative to polysome (P) calculated. This run-off rate represents the shift in S:P between the two time points, which is proportional to elongation speed. Data are average ± s.e.m. (n≥3 biological replicates per group; *p-value≤0.05, Mann Whitney U test). Also see Supplemental Figure 7.

Figure 4: mTORC1 signalling via eEF2K controls intestinal proliferation following Wnt-signalling

a) Graphical representation of findings and boxplots showing that murine intestinal regeneration following irradiation implicates the mTORC1-S6K-eEF2K axis in Wnt-driven proliferation. Animals were exposed to 14Gy γ-irradiation, and intestinal regeneration was calculated 72hrs after exposure, by examining the number and size of regenerating crypts, relative to WT regenerating intestines. Whiskers are max and min, black line is median (n=6 per group; *p-value<0.05, NS: not significant, Mann-Whitney U test); **b+c)** Representative H+E and boxplot showing *Eef2k* deletion confers resistance to 10mg/kg rapamycin treatment, 96hrs after *Apc* deletion. Treatment began 24hrs after induction. Red bar is graphical representation of crypt size. Whiskers are max and min, black line is median (n=3 biological replicates per group; *p-value<0.05, Mann-Whitney U test); **d)** qRT-PCR of intestinal epithelial cells using primers for *Cdk4*, *Cdk6*, *Ccnd1*, *Ccnd2* and *Ccnd3*. *Ccnd3* is not regulated at the transcriptional level. Data were normalised to *Gapdh*. Data are average ± s.e.m. (n=3 biological replicates per group, *p-value≤0.05, NS: not significant, Mann Whitney U test); **e)** Western blot analysis of intestinal epithelial cells from each group.

Antibodies to CDK4, CDK6, Cyclin D1, Cyclin D2, Cyclin D3 and β-actin are shown. Each well represents a different mouse from the relevant group, and are the same samples used for the qRT-PCR. Scale bar = 100μm.

Extended Data Fig. 1: mTORC1 is activated following Wnt-signal and its inhibition does not affect homeostasis

a) Reptesentative IHC of phospho-rpS6 and phospho-4EBP1 show mTORC1 activity during intestinal regeneration, 72hrs after 14Gy γ-irradiation; **b+c)** boxplots demonstrating that 72hrs of 10mg/kg rapamycin treatment does not alter mitosis or apoptosis in normal intestinal crypts. Whiskers are max and min, black line is median (n=4 per group; NS: not significant, Mann-Whitney U test); **d)** Intestines imaged on OV100 microscope, 96hrs post induction, for RFP. Tissue without the ROSA-tdRFP reporter (labelled Neg Control) show no RFP positivity, while the positive control and Raptor fl/fl intestines show high RFP positivity; **e+f)** boxplot showing that Raptor deletion does not affect mitosis or apoptosis rates in intestinal crypts, 96hrs after induction. Whiskers are max and min, black line is median (n=4 per group; NS: not significant, Mann-Whitney U test). Scale bar = 100μm

Extended Data Fig. 2: Raptor deletion is maintained in the small intestine

a) Representative IHC of phospho-rpS6 and phospho-4EBP1 shows maintained loss of mTORC1 signalling 400+ days after Raptor deletion. Arrows indicate unrecombined escaper crypts that still show active mTORC1 signalling; **b+c)** boxplots showing that mitosis and apoptosis are unchanged 400+ days after Raptor deletion. Mitosis and apoptosis were counted on H+E sections and are quantified as percent mitosis or apoptosis per crypt. Whiskers are max and min, black line is median (n=5 per group; NS: not significant, Mann-Whitney U test). Scale bar = 100μm

Extended Data Fig. 3: Wnt-signalling is still active after Raptor deletion

a+b) Representative IHC of MYC and β-catenin showing high MYC levels and nuclear localisation of β-catenin 96hrs after *Apc* and *Apc/*Raptor deletion, demonstrating active Wnt-signalling. Nuclear staining (as opposed to membranous staining) of β-catenin is indicative of active Wnt-signalling; Scale bar = 100μm

Extended Data Fig. 4: Rapamycin treatment causes regression of established tumours

a) Kaplan-Meyer survival curve of $Apc^{Min/+}$ mice treated with rapamycin when showing signs of intestinal neoplasia. 10mg/kg rapamycin treatment started when mice showed signs of intestinal disease, and was withdrawn after 30 days. Animals continued to be observed until signs of intestinal neoplasia. Death of animals in the rapamycin group almost always occurred following rapamycin withdrawal. (n=8 per group, ***p-value≤0.001, Log Rank test); **b)** boxplot showing that 72hr 10mg/kg rapamycin treatment causes an increase in Lysozyme positive cells in tumours. Percent Lysozyme positivity within tumours was calculated using Image J software (http://imagej.nih.gov/ij/). Whiskers are max and min, black line is median (10 tumours from each of 5 mice per group were measured, **p-value≤0.014, Mann-Whitney U test); **c)** boxplot showing that 72hrs 10mg/kg rapamycin treatment causes a decrease in BrdU positivity within tumours. Percent BrdU positivity within tumours was calculated using Image J software. Whiskers are max and min, black line is median (10 tumours from each of 5 mice per group were measured, **p-value≤0.021, Mann-Whitney U test); **d)** Representative IHC of Lysozyme, showing a lack of Lysozyme positive paneth cells in remaining cystic tumours after 30 days of 10mg/kg rapamycin treatment; Scale bar = 100μm.

Extended Data Fig. 5: IHC following rapamycin treatment

a) Representative IHC of p21, p16, and p53 after 6hrs and 72hrs of 10mg/kg rapamycin treatment. Staining shows no induction of these proteins in tumours following rapamycin treatment; **b)** Representative IHC for LGR5 GFP showing high numbers of LGR5-positive cells after 7 and 30 days of 10mg/kg daily rapamycin treatment. Scale bar = 100μm

Extended Data Fig. 6: Raptor deletion in the intestinal crypt

a) Graph showing that Raptor deletion prevents intestinal crypts from growing *ex vivo*. Intestinal crypts were isolated and cultured as previously described[17], 96hrs after *Cre* induction. Number of viable organoids was counted by eye 72hrs after crypt isolation. Data are average ± s.d. (n=3 biological replicates per group).

Extended Data Fig. 7: Apc deletion increases translational elongation rates

a) Representative polysome profiles from wild-type *ex vivo* crypts incubated with harringtonine for 0 seconds (left) and 180 seconds (right) prior to harvest. **b)** The areas under the sub-polysome (40S, 60S and 80S) and polysome sections as indicated by the dashed lines in a) were quantified and expressed as a percentage of their sum. Data in the bar graph is the average ± s.e.m (n=3 per time point). **c)** and **d)** show data for *Apc* deleted crypts as for wild-type in a) and b). (n=3 biological replicates).

Extended Data Fig. 8: Cycloheximide treatment phenocopies rapamycin treatment

a) Representative H+E showing that 35mg/kg cycloheximide treatment phenocopies rapamycin treatment 96hrs after *Apc* deletion. Treatment began 24hrs after induction; **b)** Representative IHC for BrdU showing a loss of proliferation in tumours after 72hrs of 35mg/kg cycloheximide treatment. Arrow highlights normal proliferating crypts. Scale bar = 100μm

Extended Data Fig. 9: S6k deletion decreases intestinal regeneration

Graphical representation of findings, and boxplot showing that murine intestinal regeneration following irradiation is dependent on S6K. Animals were exposed to 14Gy γ-irradiation, and intestinal regeneration was calculated 72hrs after exposure by counting the number of viable crypts and multiplying that by the average size of the regenerating crypts. Relative regeneration was calculated by comparing each group to WT regeneration. Rapamycin treatment arm is reproduced from Fig.4 for visual clarity. Whiskers are max and min, black line is median (n=6 per group, *p-value=0.034, Mann Whitney U test).

Extended Data Fig. 10: Eef2k deletion drives resistance to rapamycin

a) Representative IHC of phospho-eEF2 and phospho-S6 in WT, *Apc*-deficient and *Apc*- and *Eef2k*-deficient (with and without 72hrs 10mg/kg rapamycin treatment) shows that rapamycin is unable to induce eEF2 phosphorylation in the absence of eEF2K. Scale bar = 100μm

Extended Data Fig. 11: Cyclin D3 is regulated at the level of elongation

a) Representative IHC of $Apc^{fl/fl}$ intestines with and without *Eef2k* deletion. Antibodies to eEF2K, phospho-S6, and Cyclin D3 are shown. Following *Eef2k* KO, Cyclin D3 levels are no longer decreased upon 10mg/kg rapamycin treatment; **b)** boxplot showing the number of Cyclin D3 positive cells per crypt, 96hrs after *Apc* deletion, with and without 10mg/kg rapamycin treatment. Graph shows that in *Eef2k* KO animals, rapamycin no longer reduced Cyclin D3 levels (n≥3 biological replicates per group; *p-value≤0.05, Mann Whitney U test); **c)** western blot analysis of intestinal epithelial cells from $Apc^{fl/fl}$ and $Apc^{fl/fl}$ *Eef2k KO,* with and without 10mg/kg rapamycin . Antibodies to eEF2K, phospho-S6, Cyclin D3 and β-actin are shown. Each well represents a different mouse from the relevant group. Cyclin D3 levels are no longer reduced following *Eef2k* deletion. Scale bar = 100μm.

Extended Data Fig. 12: Ribosomes elongate faster on Ccnd3 following Apc deletion

The ribosome run-off rate of various messages was measured as in Figure 3. Elongation of *Ccnd3* was significantly increased, while *Actb*, *Rps21*, *Rps6* and *Ccnd1* remain unchanged. Data are average ± s.e.m. ($n \geq 3$ biological replicates per group; *p-value$\leq$0.05, Mann Whitney U test).

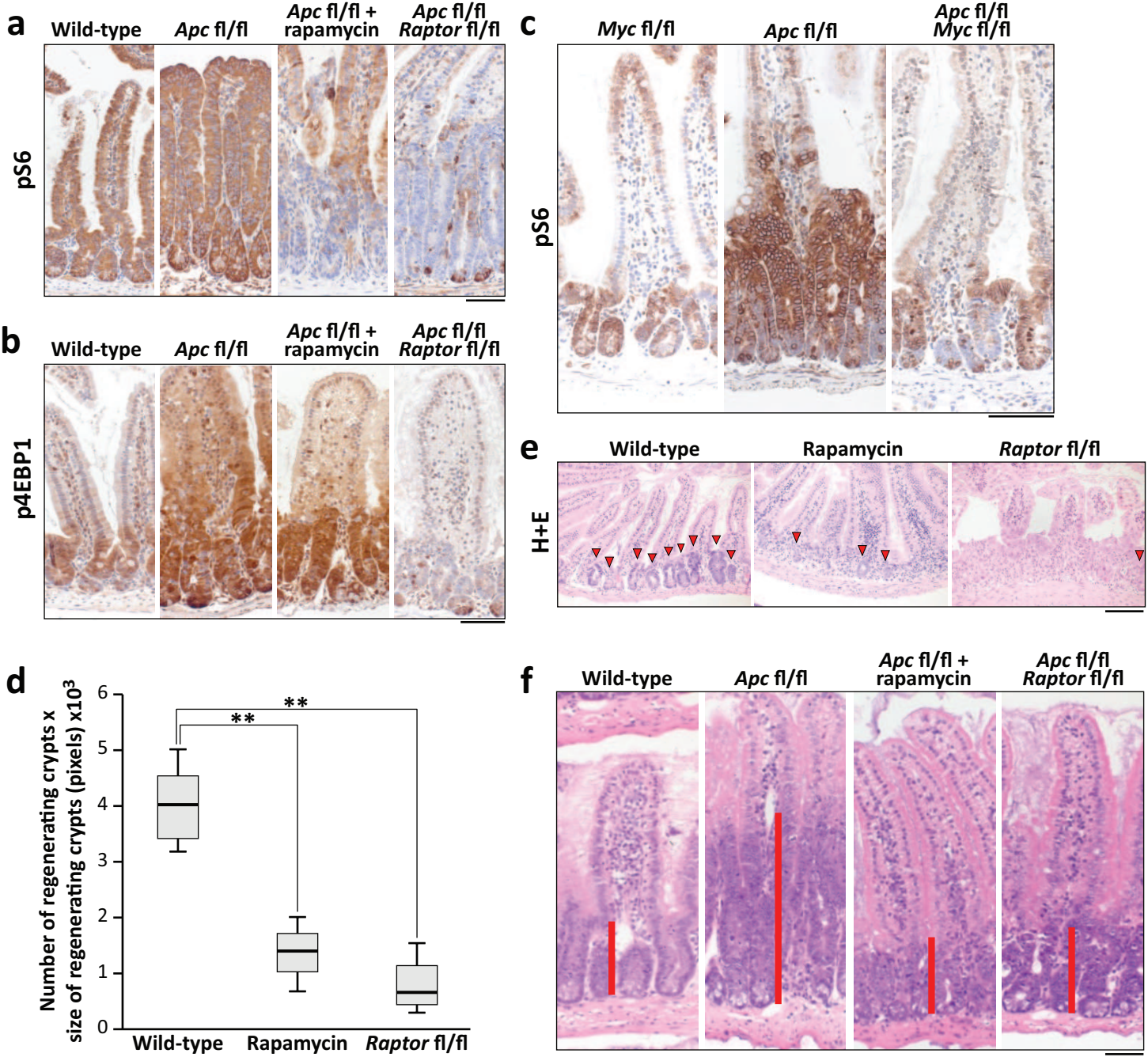
a
Wild-type
Apc fl/fl
Apc fl/fl + rapamycin
Apc fl/fl Raptor fl/fl
pS6
b
Wild-type
Apc fl/fl
Apc fl/fl + rapamycin
Apc fl/fl Raptor fl/fl
p4EBP1
c
Myc fl/fl
Apc fl/fl
Apc fl/fl Myc fl/fl
pS6
e
Wild-type
Rapamycin
Raptor fl/fl
H+E
d
Number of regenerating crypts x size of regenerating crypts (pixels) x10^3
0
1
2
3
4
5
6
**
**
Wild-type
Rapamycin
Raptor fl/fl
f
Wild-type
Apc fl/fl
Apc fl/fl + rapamycin
Apc fl/fl Raptor fl/fl

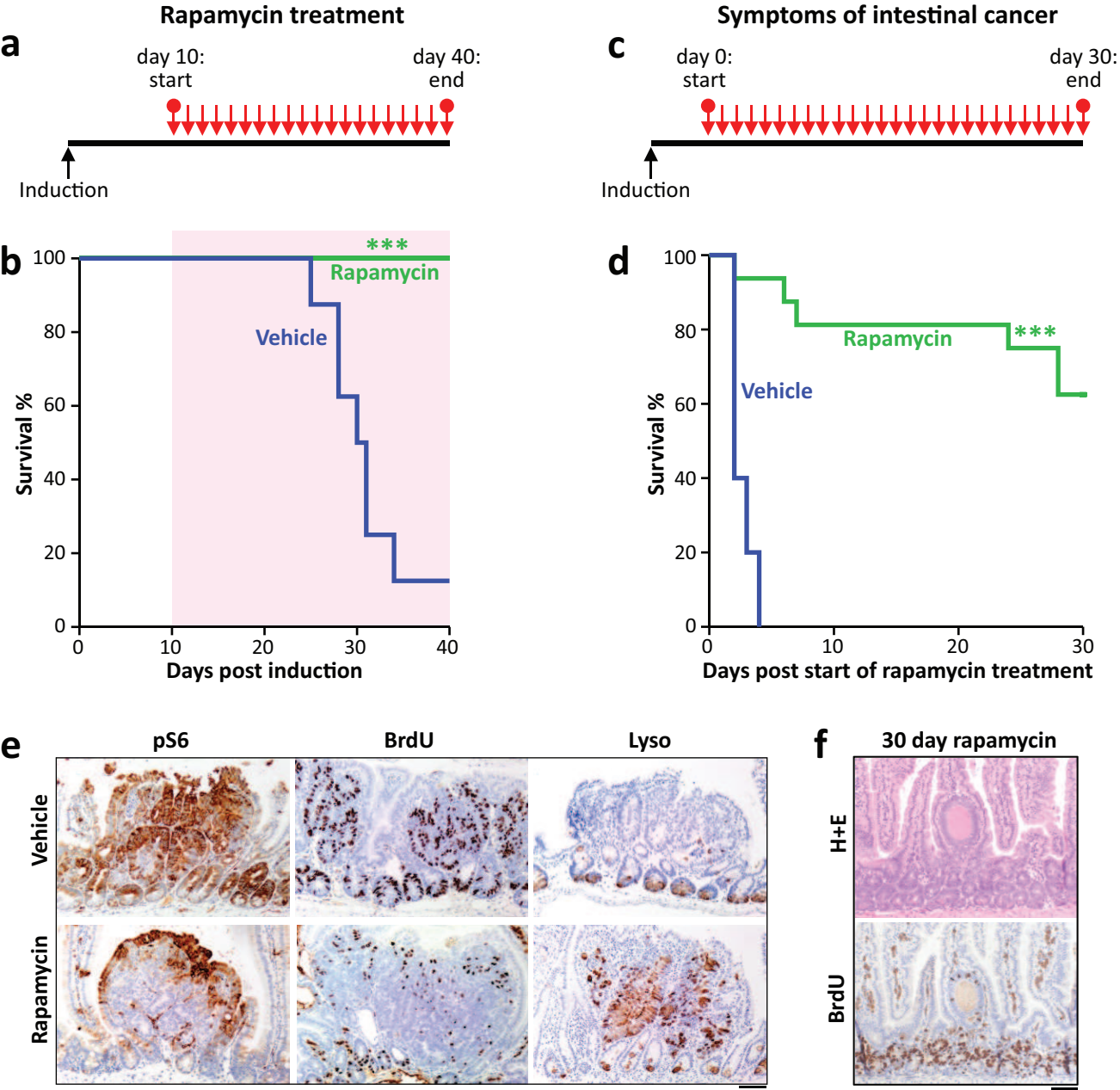
Rapamycin treatment
a
day 10:
start
day 40:
end
Induction
Symptoms of intestinal cancer
c
day 0:
start
day 30:
end
Induction
b
***
Rapamycin
Vehicle
Survival %
Days post induction
d
Rapamycin
***
Vehicle
Survival %
Days post start of rapamycin treatment
e
pS6
BrdU
Lyso
Vehicle
Rapamycin
f
30 day rapamycin
H+E
BrdU

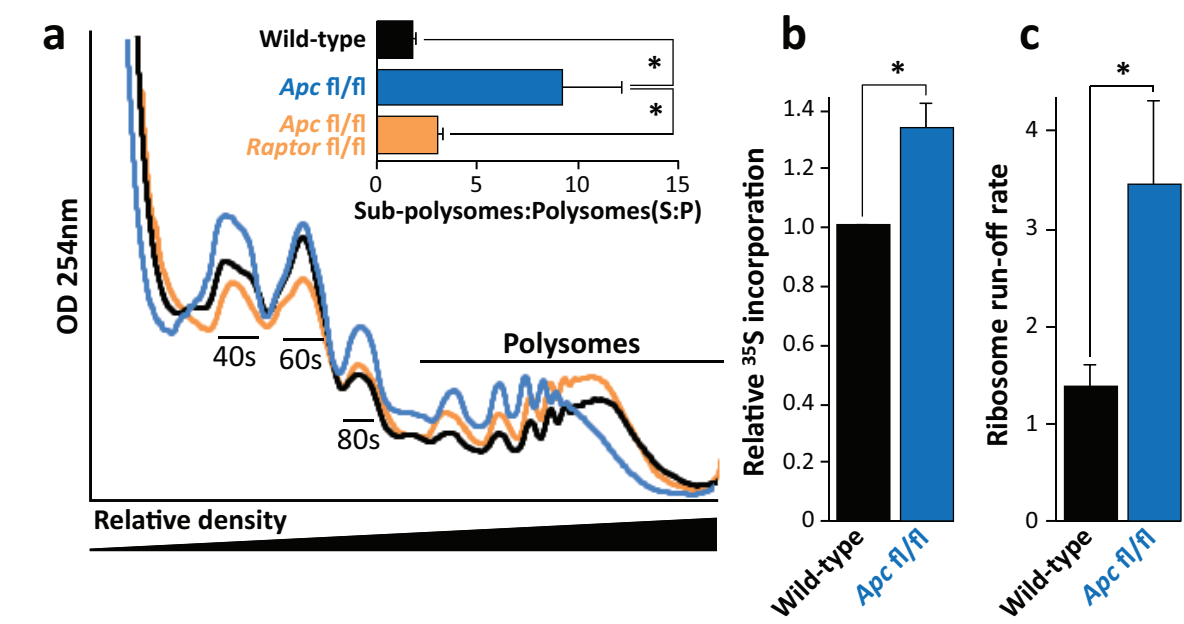
a
Wild-type
Apc fl/fl
Apc fl/fl
Raptor fl/fl
*
*
0
5
10
15
Sub-polysomes:Polysomes(S:P)
OD 254nm
40s
60s
80s
Polysomes
Relative density
b
*
Relative 35S incorporation
1.4
1.2
1.0
0.8
0.6
0.4
0.2
0
Wild-type
Apc fl/fl
c
*
Ribosome run-off rate
4
3
2
1
0
Wild-type
Apc fl/fl

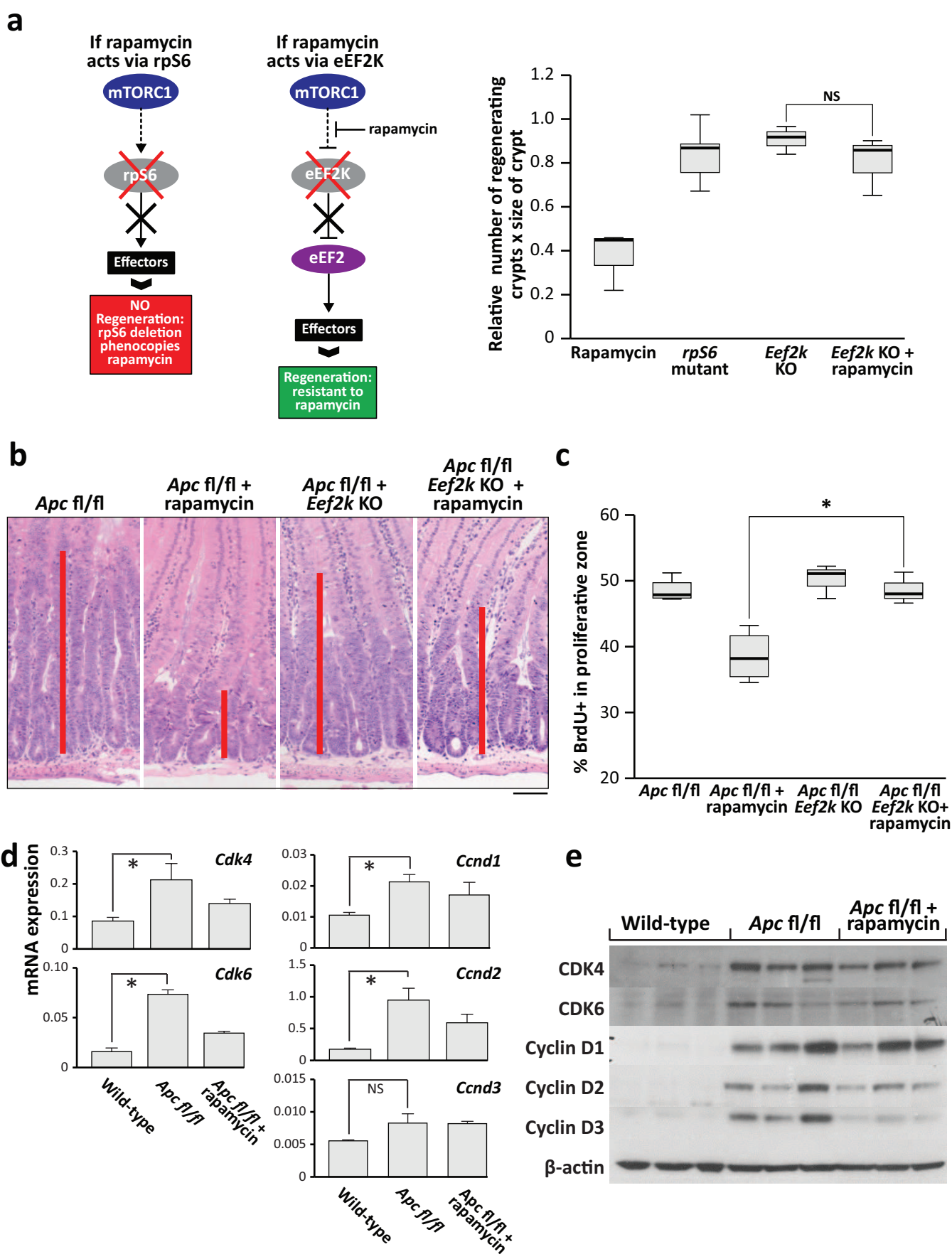
a
If rapamycin acts via rpS6
mTORC1
rpS6
Effectors
NO Regeneration: rpS6 deletion phenocopies rapamycin
If rapamycin acts via eEF2K
mTORC1
rapamycin
eEF2K
eEF2
Effectors
Regeneration: resistant to rapamycin
Relative number of regenerating crypts x size of crypt
1.2
1.0
0.8
0.6
0.4
0.2
0
NS
Rapamycin
rpS6 mutant
Eef2k KO
Eef2k KO + rapamycin
b
Apc fl/fl
Apc fl/fl + rapamycin
Apc fl/fl + Eef2k KO
Apc fl/fl Eef2k KO + rapamycin
c
% BrdU+ in proliferative zone
60
50
40
30
20
*
Apc fl/fl
Apc fl/fl + rapamycin
Apc fl/fl Eef2k KO
Apc fl/fl Eef2k KO+ rapamycin
d
mRNA expression
Cdk4
Cdk6
Ccnd1
Ccnd2
Ccnd3
NS
Wild-type
Apc fl/fl
Apc fl/fl + rapamycin
e
Wild-type
Apc fl/fl
Apc fl/fl + rapamycin
CDK4
CDK6
Cyclin D1
Cyclin D2
Cyclin D3
β-actin